Eur. Phys. J. A **25**, 257–261 (2005)
DOI 10.1140/epja/i2005-10122-3

THE EUROPEAN PHYSICAL JOURNAL A

Nuclear pairing from chiral pion-nucleon dynamics

N. Kaiser[1], T. Nikšić[2], and D. Vretenar[2,a]

[1] Physik-Department der Technischen Universität München, D-85748 Garching, Germany
[2] Physics Department, Faculty of Science, University of Zagreb, Zagreb, Croatia

Received: 25 February 2005 / Revised version: 10 May 2005 /
Published online: 29 August 2005 –
Communicated by G. Orlandini

Abstract. We use a recently improved version of the chiral nucleon-nucleon potential at next-to-next-to-leading order to calculate the $^1S_0$ pairing gap in isospin-symmetric nuclear matter. The pairing potential consists of the long-range one- and two-pion exchange terms and two short-distance NN-contact couplings. We find that the inclusion of the two-pion exchange at next-to-next-to-leading order reduces substantially the cutoff dependence of the $^1S_0$ pairing gap determined by solving a regularised BCS equation. Our results are close to those obtained with the universal low-momentum nucleon-nucleon potential $V_{\text{low-}k}$ or the phenomenological Gogny D1S force.

PACS. 13.75.Gx Pion-baryon interactions – 21.30.Cb Nuclear forces in vacuum – 21.30.Fe Forces in hadronic systems and effective interactions – 21.60.-n Nuclear structure models and methods

The self-consistent mean-field framework, extended to take into account the most important correlations, provides at present the only viable microscopic description of structure phenomena in light and heavy nuclei over the entire periodic table. A broad range of successful applications to nuclear structure and low-energy dynamics characterizes mean-field models based on the Gogny interaction, the Skyrme energy functional, and the relativistic meson-exchange effective Lagrangian [1,2]. The effective forces used in these models contain a moderate number of free parameters that are adjusted to global properties of a small set of spherical and stable nuclei, rather than to the observables of free NN-scattering. In other words, even though the global effective nuclear interactions model the interaction between nucleons in the nuclear medium, they are not necessarily related to any particular NN-potential.

On the other hand, a new approach in which nuclear interactions are formulated in terms of effective field theory [3–5] has recently been developed. Its key element is a separation of long- and short-distance dynamics and an ordering scheme in powers of small momenta. The NN-potential, as constructed in chiral perturbation theory, consists of the long-range contributions generated by one-, two- and three-pion exchanges [6,7], and a set of contact-terms encoding the short-distance dynamics. The associated low-energy constants are adjusted to empirical NN-phase shifts and deuteron properties. It has also been shown that their values can be understood in terms of the heavy-mass resonance exchanges [8]. Furthermore, when isospin-breaking corrections are systematically included, the chiral NN-potential reaches almost the same accuracy as the more phenomenological "high-precision" NN-potentials. This has been demonstrated by numerous calculations of two- and few-nucleon systems [7].

Another line of approach, developed by the Stony Brook group, applies renormalisation group arguments to eliminate the high-momentum components from phase-shift equivalent NN-potentials. By integrating out the high-momentum components below a cutoff scale $\Lambda \approx 2\ \text{fm}^{-1}$, a universal low-momentum NN-potential $V_{\text{low-}k}$ emerges [9]. Consequently, this potential operates only in the subspace of nucleon states with momenta $p \leq \Lambda$. The pairing properties of nuclear matter derived from the potential $V_{\text{low-}k}$ have been investigated recently in ref. [10]. Good agreement with the phenomenological Gogny pairing interaction has been found for a wide range of nuclear densities. Calculations of nuclear matter have also been performed using the potential $V_{\text{low-}k}$. Whereas the Brueckner-Hartree-Fock approximation applied to this two-body potential leads to unsatisfactory results [11], reasonable saturation properties of nuclear matter can be obtained by including the effects of the leading chiral three-nucleon interaction [12]. These findings are consistent with the fact that nuclear pairing is primarily a low-density phenomenon. The maximum of the $^1S_0$ pairing gap typically occurs at a density $\rho \approx \rho_0/4$, where $\rho_0 \simeq 0.16\,\text{fm}^{-3}$ denotes the nuclear-matter equilibrium density.

The purpose of the present paper is to investigate the pairing properties of the chiral NN-potential. Quite generally, the momentum- and density-dependent pairing field

[a] e-mail: vretenar@phy.hr

$\Delta(k, k_{\rm f})$ in infinite nuclear matter is determined by the solution of the BCS gap equation

$$\Delta(k,k_{\rm f}) = -\frac{1}{4\pi^2} \times \int_0^\infty \frac{p^2 V(p,k)\Delta(p,k_{\rm f})}{\sqrt{[\mathcal{E}(p,k_{\rm f})-\mathcal{E}(k_{\rm f},k_{\rm f})]^2+\Delta(p,k_{\rm f})^2}}\,{\rm d}p\,. \quad (1)$$

Here, $V(p,k)$ represents the off-shell pairing potential in momentum space, and $\mathcal{E}(p,k_{\rm f})$ is the quasiparticle energy with $\mathcal{E}(k_{\rm f},k_{\rm f})$ the corresponding Fermi energy.

The effective force in the pairing channel is generated by the sum of all particle-particle irreducible Feynman diagrams [13–15]. In most application to nuclear and neutron matter, however, only the lowest-order term, which corresponds to the bare NN-interaction, is retained [16]. Terms of higher order in the effective pairing interaction represent screening corrections to the bare force, caused by medium polarization effects. Numerous studies have shown that polarization effects can have a pronounced influence on the calculated values of the pairing gaps (see, for instance, refs. [17–19]). The influence of both the vertex corrections to the pairing interaction, and the self-energy corrections, on the properties of $^1S_0$ pairing in neutron and nuclear matter has recently been studied in the framework of the generalized gap equation [20,21]. It has been found that the two effects lead to a strong suppression of the pairing correlations in neutron matter (the pairing gap is reduced by more than 50% with respect to the BCS prediction), whereas they cancel each other out to a large extent in isospin-symmetric nuclear matter[1]. The pairing correlation energy in finite nuclei can be calculated in the local density approximation (LDA). LDA calculations with the Gogny D1 force have been compared with exact Hartree-Fock-Bogoliubov (HFB) calculations of the pairing correlation energy for many spherical nuclei [23]. Except for shell effects, the results of these calculations are in close agreement with each other, and thus one should not expect large effects from medium corrections not included in the BCS limit.

For the pairing potential $V(p,k)$ we employ the improved version of the chiral NN-potential derived in refs. [24,25]. An overly strong medium-range attraction in the isoscalar central part of the chiral two-pion exchange at the next-to-next-to-leading order, present in earlier versions of the chiral NN-potential [5], has been removed by using the spectral function regularization method. Essentially, this means that only $\pi\pi$-intermediate states of invariant mass below a scale $\tilde{\Lambda}$ (where the chiral effective field theory is applicable) are taken into account in the pion-loop integrals, while shorter-range contributions should be represented by NN-contact interactions. At this stage medium modifications of the pairing potential $V(p,k)$ are not taken into account. In the chiral effective field theory these arise from additional (in-medium) loops, which are suppressed at low Fermi momenta.

The (bare) chiral NN-potential used in the present study consists of the one-pion exchange term, the NN-contact interaction, and the irreducible two-pion exchange term

$$V(p,k) = V^{(1\pi)}(p,k) + V^{(ct)}(p,k) + V^{(2\pi)}(p,k)\,. \quad (2)$$

This approximation for the two-nucleon potential is valid for small values of the momenta p and k and it breaks down for momenta above the chiral-symmetry-breaking scale. An additional cutoff Λ, included by multiplying the potential $V(p,k)$ with a regulator function $f^\Lambda(p)$ [5],

$$V(p,k) \to f^\Lambda(p) V(p,k) f^\Lambda(k)\,, \quad (3)$$

prevents the growth of the potential with increasing momenta p and k. Following the procedure of ref. [25], we employ the exponential regulator function

$$f^\Lambda(p) = \exp(-p^6/\Lambda^6)\,. \quad (4)$$

Even though both cutoff parameters, $\tilde{\Lambda}$ and Λ, are introduced to remove high-momentum components of the interacting nucleon and pion fields, their roles are different. The inclusion of $\tilde{\Lambda}$ removes the short-distance portion of the two-pion exchange component, whereas the cutoff Λ ensures that high-momentum nucleon states do not contribute to the scattering process. If all terms in the EFT expansion are included, low-energy observables should not depend on the cutoff parameters. In practice, however, the expansion is always truncated at some order. Consequently, the observables depend on the cutoffs to some extent, but this dependence should become weaker when higher-order terms are included. Unless stated otherwise, we use the value $\Lambda = 550$ MeV in the following calculations.

The one-pion exchange contribution in the S-wave channel reads

$$V^{(1\pi)}(p,k) = \frac{g_A^2}{2f_\pi^2}\left\{1 - \frac{m_\pi^2}{4pk}\ln\frac{m_\pi^2+(p+k)^2}{m_\pi^2+(p-k)^2}\right\}. \quad (5)$$

The following numerical values are used for the nucleon axial vector coupling constant g_A, the weak pion decay constant f_π, and the pion mass m_π: $g_A = 1.3$, $f_\pi = 92.4\,{\rm MeV}$, $m_\pi = 135\,{\rm MeV}$.

The contact interaction comes from four-nucleon contact-operators without and with two derivatives

$$V^{(ct)}(p,k) = \frac{\widetilde{C}_{^1S_0}}{2\pi} + \frac{C_{^1S_0}}{2\pi}(p^2+k^2)\,. \quad (6)$$

For each choice of the cutoff parameters, $\tilde{\Lambda}$ and Λ, the low-energy constants $\widetilde{C}_{^1S_0}$ and $C_{^1S_0}$ are determined by a fit to the $^1S_0$ phase-shifts below the inelastic $NN\pi$-threshold [25]. The cutoff dependence entering through the regulator function $f_\Lambda(p)$ is then to a large extent cancelled by that of the running low-energy constants $\widetilde{C}_{^1S_0}$

[1] The situation has, however, been confused by the recent results of ref. [22], where an enormous additional attraction in symmetric nuclear matter has been obtained from resuming the particle-hole bubble chain. It has therefore been argued that the employed many-body approach is not converging and a more controlled scheme like variational theory may be in order.

and $C_{^1S_0}$. In the present calculation we employ the central values of the low-energy constants at next-to-leading order (NLO) and next-to-next-to-leading order (NNLO) listed in table 4 of ref. [25]. These particular values of the low-energy constants have been adjusted for $\tilde{\Lambda} = 600\,\mathrm{MeV}$ and $\Lambda = 550\,\mathrm{MeV}$.

The irreducible two-pion exchange contribution is most conveniently calculated via a twice subtracted dispersion relation

$$V^{(2\pi)}(p,k) = \frac{1}{\pi}\int_{2m_\pi}^{\tilde{\Lambda}} \mathrm{d}\mu\, \mathrm{Im}[V_C + W_C - 2\mu^2 V_T - 2\mu^2 W_T] \times\left\{\frac{4}{\mu} - \frac{4}{\mu^3}(p^2+k^2) - \frac{\mu}{pk}\ln\frac{\mu^2+(p+k)^2}{\mu^2+(p-k)^2}\right\}. \quad (7)$$

Here, $\mathrm{Im}V_C$, $\mathrm{Im}W_C$, $\mathrm{Im}V_T$, and $\mathrm{Im}W_T$ are the imaginary parts of the isoscalar central, isovector central, isoscalar tensor, and isovector tensor NN-amplitudes. The weighting function in curly brackets originates from projecting the NN-potential onto the spin-singlet S-wave. The cutoff parameter $\tilde{\Lambda}$, which restricts the spectral functions calculated in chiral perturbation theory to their low-energy domain of validity, is kept fixed throughout this work at $\tilde{\Lambda} = 600$ MeV. The imaginary parts of the isovector central and isoscalar tensor NN-amplitudes contribute at NLO, while the imaginary parts of the isoscalar central and isovector tensor NN-amplitudes contribute at NNLO in the chiral expansion. Explicitly, the spectral functions corresponding to the two-pion exchange at NLO read

$$\mathrm{Im}W_C(i\mu) = \frac{\sqrt{\mu^2-4m_\pi^2}}{3\pi\mu(4f_\pi)^4}\bigg[4m_\pi^2(1+4g_A^2-5g_A^4) + \mu^2(23g_A^4-10g_A^2-1) + \frac{48g_A^4m_\pi^4}{\mu^2-4m_\pi^2}\bigg], \quad (8)$$

$$\mathrm{Im}V_T(i\mu) = -\frac{6g_A^4\sqrt{\mu^2-4m_\pi^2}}{\pi\mu(4f_\pi)^4}, \quad (9)$$

and at NNLO

$$\mathrm{Im}V_C(i\mu) = \frac{3g_A^2}{64\mu f_\pi^4}\Big[(4c_1-2c_3)m_\pi^2 + c_3\,\mu^2\Big](2m_\pi^2-\mu^2), \quad (10)$$

$$\mathrm{Im}W_T(i\mu) = \frac{g_A^2c_4}{128\mu f_\pi^4}(4m_\pi^2-\mu^2), \quad (11)$$

with the low-energy constants: $c_1 = -0.81\,\mathrm{GeV}^{-1}$, $c_3 = -3.40\,\mathrm{GeV}^{-1}$, and $c_4 = 3.40\,\mathrm{GeV}^{-1}$ [24–26]. The two relatively large low-energy constants $c_{3,4}$ represent mainly effects from excitations of virtual $\Delta(1232)$-isobars. For the single-particle spectrum which enters the gap equation (1), we employ the simple quadratic form

$$\mathcal{E}(p,k_\mathrm{f}) - \mathcal{E}(k_\mathrm{f},k_\mathrm{f}) = \frac{p^2-k_\mathrm{f}^2}{2M^*(k_\mathrm{f})}. \quad (12)$$

Such an approximation is sufficient since momenta p around k_f give the dominant contribution to the integral in eq. (1). The effective nucleon mass $M^*(k_\mathrm{f})$ is taken from a recent three-loop calculation of nuclear matter including 2π-exchange with virtual $\Delta(1232)$-isobar excitation [27]. Note that in our pairing potential $V^{(2\pi)}(p,k)$ the same $\pi N\Delta$-dynamics is effectively represented by the low-energy constants $c_{3,4}$.

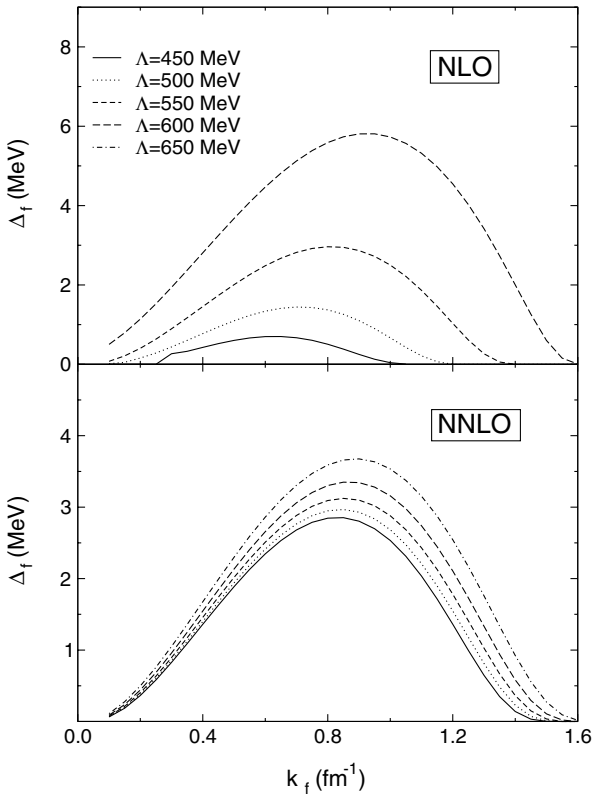

Fig. 1. Pairing gap at the Fermi surface $\Delta_\mathrm{f} \equiv \Delta(k_\mathrm{f},k_\mathrm{f})$ as a function of the Fermi momentum, for different values of the cutoff Λ, at NLO (upper panel) and NNLO (lower panel).

As we have already mentioned, low-energy observables should not depend sensitively on the value of the cutoff Λ. In addition, this dependence should become weaker when higher-order terms in the small momentum expansion are included. To verify this feature, we have calculated the pairing gaps $\Delta_\mathrm{f} \equiv \Delta(k_\mathrm{f},k_\mathrm{f})$ in isospin-symmetric nuclear matter for several cutoffs Λ between 450 MeV and 650 MeV. For the low-energy constants $\widetilde{C}_{^1S_0}$ and $C_{^1S_0}$ we have used the central values listed in table 4 of ref. [25], and the spectral function cutoff $\tilde{\Lambda}$ has been fixed at $\tilde{\Lambda} = 600$ MeV. Notice that no attempt has been made to readjust the LECs when changing the cutoff Λ. The results are displayed in fig. 1. At NLO the pairing gap depends strongly on the value of Λ. When increasing the cutoff from $\Lambda = 450$ MeV to $\Lambda = 600\,\mathrm{MeV}$, the maximum value of the pairing gap increases from $\Delta_\mathrm{f}^\mathrm{max} = 0.7\,\mathrm{MeV}$ to $\Delta_\mathrm{f}^\mathrm{max} = 5.8\,\mathrm{MeV}$, and the value of the Fermi momentum for which the pairing gap reaches its maximum changes from $k_\mathrm{f}^\mathrm{max} = 0.65\,\mathrm{fm}^{-1}$ to $k_\mathrm{f}^\mathrm{max} = 0.95\,\mathrm{fm}^{-1}$. For $\Lambda = 650\,\mathrm{MeV}$ the maximum value of the gap is well above 10 MeV and the calculation obviously diverges. The results are much improved at NNLO. The position of the maximum changes very little with increasing Λ and the

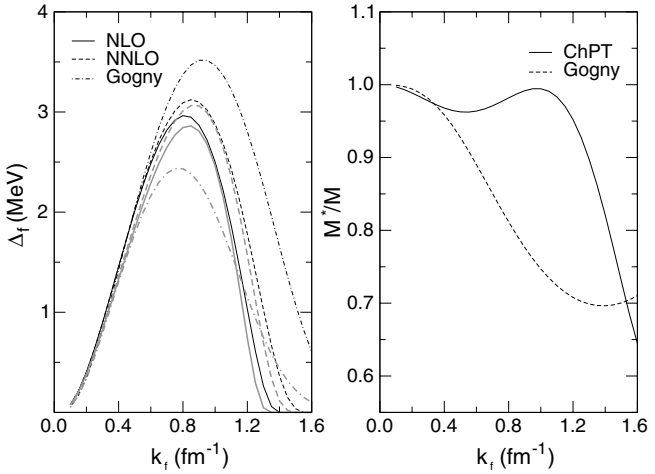

Fig. 2. Pairing gaps at the Fermi surface $\Delta_{\rm f} = \Delta(k_{\rm f}, k_{\rm f})$ in isospin-symmetric nuclear matter, calculated with the chiral NN-potential (2) at NLO and NNLO (for $\Lambda = 550\,\mathrm{MeV}$), and with the effective Gogny interaction D1S [28]. The heavy and light curves refer to calculations with noninteracting and medium-modified single-particle spectra, respectively. The panel on the right illustrates the density dependence of the effective nucleon mass for the Gogny interaction and for the chiral approach to nuclear matter of ref. [27].

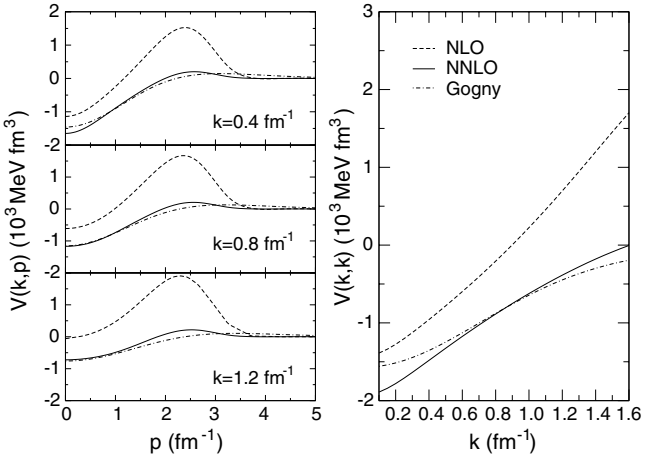

Fig. 3. Momentum dependence of the pairing potential $V(p,k)$: chiral NN-potential at NLO and NNLO, and the Gogny DS1 interaction, for three different values of the momentum $k = 0.4, 0.8, 1.2$ fm^{-1}. In the panel on the right the corresponding diagonal matrix elements $V(k,k)$ are shown as functions of the momentum k.

value of the pairing gap at maximum increases less than 0.8 MeV between $\Lambda = 450\,\mathrm{MeV}$ and $\Lambda = 650\,\mathrm{MeV}$. Since the gap at the Fermi surface is very sensitive to changes in the effective pairing potential, this indicates reasonable convergence for the EFT expansion. The improved description of the pairing gap, when going from NLO to NNLO, is naturally correlated with the improved description of the NN-phase shifts [5,16].

In the left panel of fig. 2 we compare the density dependence of the pairing gaps in nuclear matter, calculated by employing the chiral NN-potential and with the effective Gogny interaction. The solid and the dashed curves correspond to the chiral potential at NLO and NNLO, respectively. The dash-dotted curve is the pairing gap calculated with the D1S Gogny interaction [28]. Similar to the analysis of ref. [10], where the Gogny pairing gaps were compared with those calculated with the low-momentum $V_{\text{low-}k}$ interaction extracted from realistic forces, we have calculated the pairing gaps using both the noninteracting single-particle spectra (heavy curves), and the medium-modified single-particle spectra (light curves). The medium-modified single-particle spectra are computed in the Hartree-Fock approximation for the Gogny interaction, and by using eq. (12) for the chiral NN-potential. First, we notice that for the noninteracting single-particle spectra there is a qualitative and, at low densities $k_{\rm f} \leq 0.8\,\mathrm{fm}^{-1}$, even a quantitative agreement between the pairing gaps calculated with the chiral NN-potential and the effective Gogny interaction. The inclusion of the NNLO contribution increases the value of the pairing gap at maximum and shifts the position of the maximum to a slightly higher value of $k_{\rm f}$, in closer agreement with the Gogny pairing gap. For $k_{\rm f} > 1\,\mathrm{fm}^{-1}$ and closer to saturation density, we find a more pronounced difference between the Gogny pairing gap and the gaps calculated with the chiral NN-potential. This difference with respect to the Gogny pairing gap at higher densities has also been observed for other bare NN-interactions [29,30,10].

The effective nucleon mass is reduced in the nuclear medium. This results in a lower density of states around the Fermi surface and, hence, in weaker pairing correlations. The reduction of the pairing gap is much more pronounced for the Gogny effective interaction than for the chiral NN-potential. This is caused by a much stronger reduction of the effective mass for the former interaction in the relevant range of densities $0.4\,\mathrm{fm}^{-1} \leq k_{\rm f} \leq 1.2\,\mathrm{fm}^{-1}$. The effective nucleon mass $M^*(k_{\rm f})$ from the chiral three-loop calculation [27], and for the D1S Gogny effective interaction are shown in the right panel of fig. 2. The density dependence is very different in the two cases, and this means that one should not, at least on the quantitative level, compare the corresponding pairing gaps calculated with medium-modified single-nucleon spectra.

In fig. 3 we plot the momentum dependence of the pairing potentials $V(p,k)$ for three different values of the momenta: $k = 0.4,\ 0.8,\ 1.2\,\mathrm{fm}^{-1}$. While the Gogny interaction and the chiral NN-potential at NLO display only a qualitatively similar momentum dependence, the inclusion of the NNLO contributions brings the chiral NN-potential in remarkable agreement with the Gogny D1S interaction. The same is true and even more pronounced for the diagonal matrix elements $V(k,k)$ shown in the right panel of fig. 3. A similar result has been observed for the potential $V_{\text{low-}k}$ in ref. [10].

In conclusion, we have presented a study of the pairing properties of the chiral NN-potential. This potential consists of the long-range one- and two-pion exchange terms, and it includes two short-distance NN-contact terms. Our main result is that the inclusion of the two-pion exchange

at the next-to-next-to-leading order reduces substantially the cutoff dependence of the $^1S_0$ pairing gap, indicating reasonable convergence of the small momentum expansion. In addition, the inclusion of the NNLO contributions brings the chiral NN-potential in remarkable agreement with the Gogny D1S interaction (the "standard" nuclear pairing force) and the universal low-momentum potential $V_{\text{low-}k}$. Clearly, once the chiral NN-potential reaches a certain accuracy in reproducing empirical NN-phase shifts it represents also a realistic low-momentum interaction. In the future we plan to include higher-order terms in the chiral NN-potential and extend the study of the pairing properties by including medium modifications, such as the polarization effects, vertex corrections and Pauli-blocking effects. The chiral effective field theory at finite density represents a systematic framework for such extension.

We thank P. Ring for useful discussions and E. Epelbaum and S. Fritsch for supplying numerical results.

References

1. M. Bender, P.-H. Heenen, P.-G. Reinhard, Rev. Mod. Phys. **75**, 121 (2003).
2. P. Ring, Prog. Part. Nucl. Phys. **37**, 193 (1996).
3. S. Weinberg, Nucl. Phys. B **363**, 3 (1991).
4. D.B. Kaplan, M.J. Savage, M.B. Wise, Nucl. Phys. B **534**, 329 (1998).
5. E. Epelbaum, W. Glöckle, Ulf-G. Meißner, Nucl. Phys. A **671**, 295 (2000) and references therein.
6. D.R. Entem, R. Machleidt, Phys. Rev. C **68**, 041001 (2003) and references. therein.
7. E. Epelbaum, W. Glöckle, Ulf-G. Meißner, Nucl. Phys. A **747**, 362 (2005).
8. E. Epelbaum, W. Glöckle, Ulf-G. Meißner, C. Elster, Phys. Rev. C **64**, 044001 (2003).
9. S.K. Bogner, T.T.S. Kuo, A. Schwenk, Phys. Rep. **386**, 1 (2003) and references therein.
10. A. Sedrakian, T.T.S. Kuo, H. Müther, P. Schuck, Phys. Lett. B **576**, 68 (2003).
11. J. Kuckei, F. Montani, H. Müther, A. Sedrakian, Nucl. Phys. A **723**, 32 (2003).
12. S.K. Bogner, A. Schwenk, R.J. Furnstahl, A. Nogga, nucl-th/0504043.
13. A.I. Larkin, A.B. Migdal, Sov. Phys. JETP **17**, 1146 (1963).
14. W. Brenig, H. Wagner, Z. Phys. **173**, 484 (1963).
15. A.B. Migdal, *Theory of Finite Fermi Systems and Applications to Atomic Nuclei* (Interscience, New York, 1967).
16. D.J. Dean, M. Hjorth-Jensen, Rev. Mod. Phys. **75**, 607 (2003) and references therein.
17. J.W. Clark, C.-G. Källman, C.H. Yang, D.A. Chakkalakal, Phys. Lett. B **61**, 331 (1976).
18. T.L. Ainsworth, J. Wambach, D. Pines, Phys. Lett. B **222**, 173 (1989).
19. H.J. Schulze, J. Cugnon, A. Lejeune, M. Baldo, U. Lombardo, Phys. Lett. B **375**, 1 (1996).
20. C. Shen, U. Lombardo, P. Schuck, W. Zuo, N. Sandulescu, Phys. Rev. C **67**, 061302(R) (2003).
21. U. Lombardo, P. Schuck, C. Shen, Nucl. Phys. A **731**, 392 (2004).
22. C. Shen, U. Lombardo, P. Schuck, Phys. Rev. C **71**, 054301 (2005).
23. H. Kucharek, P. Ring, P. Schuck, R. Bentsson, M. Girod, Phys. Lett. B **216**, 249 (1989).
24. E. Epelbaum, W. Glöckle, U.-G. Meißner, Eur. Phys. J. A **19**, 125 (2004).
25. E. Epelbaum, W. Glöckle, U.-G. Meißner, Eur. Phys. J. A **19**, 401 (2004).
26. N. Kaiser, R. Brockmann, W. Weise, Nucl. Phys. A **625**, 758 (1997).
27. S. Fritsch, N. Kaiser, W. Weise, Nucl. Phys. A **750**, 259 (2005).
28. J.F. Berger, M. Girod, D. Gogny, Comput. Phys. Commun. **63**, 365 (1991).
29. E. Garrido, P. Sarriguren, E. Moya de Guerra, P. Schuck, Phys. Rev. C **60**, 064312 (1999).
30. M. Serra, A. Rummel, P. Ring, Phys. Rev. C **65**, 014304 (2001).